Pose2Gaze: Generating Realistic Human Gaze Behaviour from Full-body Poses using an Eye-body Coordination Model

Zhiming Hu*
University of Stuttgart

Jiahui Xu†
University of Stuttgart

Syn Schmitt‡
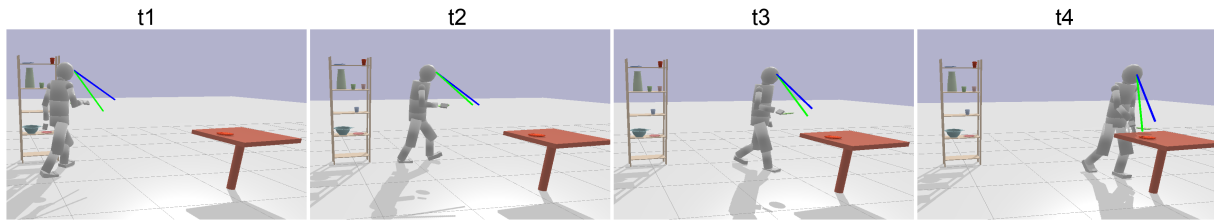University of Stuttgart

Andreas Bulling§
University of Stuttgart

Figure 1: Human body and eye movements show strong spatio-temporal coordination during everyday activities (example taken from the MoGaze dataset [26]). The green line indicates the eye gaze and the blue line denotes the head direction. We propose the first method that exploits this coordination for generating realistic human gaze behaviour for virtual avatars from full-body poses.

ABSTRACT

While generating realistic body movements, e.g., for avatars in virtual reality, is widely studied in computer vision and graphics, the generation of eye movements that exhibit realistic coordination with the body remains under-explored. We first report a comprehensive analysis of the coordination of human eye and full-body movements during everyday activities based on data from the MoGaze and GIMO datasets. We show that eye gaze has strong correlations with head directions and also full-body motions and there exists a noticeable time delay between body and eye movements. Inspired by the analyses, we then present *Pose2Gaze* – a novel eye-body coordination model that first uses a convolutional neural network and a spatio-temporal graph convolutional neural network to extract features from head directions and full-body poses respectively and then applies a convolutional neural network to generate realistic eye movements. We compare our method with state-of-the-art methods that predict eye gaze only from head movements for three different generation tasks and demonstrate that *Pose2Gaze* significantly outperforms these baselines on both datasets with an average improvement of 26.4% and 21.6% in mean angular error, respectively. Our findings underline the significant potential of cross-modal human gaze behaviour analysis and modelling.

Index Terms: Human-centered computing—Human computer interaction—Interaction paradigms—Virtual reality; Computing methodologies—Machine learning—Machine learning approaches—Neural networks;

1 INTRODUCTION

With the increasing use of augmented and virtual reality (VR) [36], the need to create virtual agents that behave realistically has grown significantly in recent years. Virtual agents that behave like humans is crucial for a variety of applications, such as online learning [31, 32], virtual interviewing and counselling [2, 7], virtual social

---

*e-mail: zhiming.hu@vis.uni-stuttgart.de
†e-mail: st170522@stud.uni-stuttgart.de
‡e-mail: schmitt@simtech.uni-stuttgart.de
§e-mail: andreas.bulling@vis.uni-stuttgart.de

interactions [29, 40], as well as large-scale virtual worlds [36]. Creating realistic behaviour is also important in character animation, e.g., in films [13]. However, previous work has mainly focused on generating realistic body movements [3, 28] despite the fact that eye movements are equally, if not even more, important in human-human encounters [41] and, as such, also for reducing the uncanny valley effect [42].

Generating realistic eye movement behaviour is challenging given the highly variable spatio-temporal dynamics of gaze allocation as well as various top-down influences, e.g., of the visual world, the agent's tasks or goals, or social norms that agents have ideally adhere to during interactions with humans [5]. Research on eye gaze prediction has revealed that eye movements are carefully coordinated with head movements and, as such, that head orientation can be used as a proxy to eye gaze direction [18, 20, 21, 45]. Consequently, previous works have mainly focused on exploiting eye-head coordination for generating eye movements [18, 20, 21].

In this work, we provide a complementary perspective and study, for the first time, eye-body coordination during everyday activities and explore the generation of realistic human gaze behaviour from full-body poses.

To this end we first report comprehensive analyses on the correlations between gaze direction and full-body movements on two publicly available datasets: MoGaze [26] and GIMO [51]. These datasets contain human eye and full-body movement data recorded using a body tracking system and a mobile eye tracker during various daily activities.To the best of our knowledge, we are first to study the coordination of eye movements and full-body movements simultaneously. Our analyses confirm that eye gaze direction is strongly correlated with head direction but also with the motions of different human body joints. We also find that there exists a noticeable time delay between full-body motions and eye movements.

Based on these findings we present *Pose2Gaze* – the first method to generate realistic human gaze behaviour from human full-body poses. At the core of our method is a novel learning-based eye-body coordination model that first uses a convolutional neural network (CNN) and a spatio-temporal graph convolutional neural network (GCN) to extract features from head directions and full-body poses respectively and then employs a convolutional neural network to generate realistic human eye gaze from the extracted features. We compare our method with state-of-the-art gaze prediction methods for three different generation tasks, i.e. generating target eye gaze from past, present, and future body poses respectively, on the

MoGaze and GIMO datasets and show that our method outperforms these baselines by a large margin on both the MoGaze (26.4% improvement) and GIMO datasets (21.6%) in terms of mean angular gaze error[1].

The specific contributions of our work are three-fold:

- We provide a comprehensive analysis of eye-body coordination in various daily activities and reveal that eye gaze is strongly correlated with head directions and also full-body motions.

- We propose *Pose2Gaze*, a novel eye-body coordination model that applies a convolutional neural network and a spatio-temporal graph convolutional neural network to extract features from head directions and full-body poses respectively and uses a convolutional neural network to generate realistic eye gaze.

- We report extensive experiments on two public datasets for three different generation tasks and demonstrate significant performance improvements over several state-of-the-art methods.

2 RELATED WORK

2.1 Human Movement Generation

Generating realistic human movements for virtual agents is an important research topic in the area of virtual reality. Some researchers focused on generating human body movements from speech signals. For example, Hasegawa et al. used recurrent neural networks (RNNs) to generate natural human full-body poses from perceptual features extracted from the input speech audio [15] while Kucherenko et al. employed autoencoder neural networks to learn latent representations for human poses and speech signals and then learned the mappings between the two representations to generate human body motions [27]. Other researchers used the text transcripts of speech to generate human poses. Specifically, Yoon et al. proposed to use a RNN-based encoder to extract features from speech text and a RNN-based decoder to generate human poses [50] while Bhattacharya et al. employed an end-to-end transformer network to generate human movements from the text transcripts of speech [3]. In addition, there also exist some works that generated human dance motions from input music and achieved good performances [30, 49]. While previous works typically focused on generating human body movements, they neglected the generation of human eye gaze, which is significant for human-human [8, 16] and human-computer interactions [9, 23, 44]. In this work, we focus on generating realistic human eye gaze directly from human full-body poses to fill this gap.

2.2 Eye-body Coordination

The coordination of human eye and body movements is an important research topic in the areas of cognitive science and human-centred computing. Many researchers focused on the coordinated movements between the eyes and the head [12, 21, 46]. Specifically, Stahl analysed the process of gaze shifts and found its amplitude to be proportional to that of head movements [46]. Fang et al. further examined eye-head coordination during visual search in a large visual field and found that eye-head coordination plays an important role in visual cognitive processing [12]. Hu et al. revealed that human eye movements are strongly correlated with head movements in both free-viewing [20, 21] and task-oriented settings [18, 19] in immersive virtual environments while Kothari et al. identified the coordination of eye and head movements in real-world daily activities [24]. Recently, some researchers went beyond eye-head coordination to investigate the correlations between eye movements and the movements of different body parts. For example, Sidenmark et al. focused on the gaze shift process in immersive virtual reality and discovered

general eye, head, and torso coordination patterns [43]. Batmaz et al. developed a VR training system based on the coordination of eye and hand movements and compared user performance in three different virtual environments [1]. Emery et al. collected a large-scale dataset that contains human eye, hand, and head movements in a virtual environment and identified the coordination of eye, hand, and head motions [11]. Randhavane et al. investigated the effectiveness of eye-gait coordination on expressing emotions and further employed gaze and gait features to generate various emotions for virtual agents [39]. However, prior works typically focused on the correlations between eye gaze and a particular body part, e.g. head, hand, or torso. In contrast, we are the first to study the coordinations of eye and full-body movements simultaneously, which paves the way for generating realistic eye gaze from full-body poses.

2.3 Eye Gaze Prediction

Eye gaze prediction is a popular research topic in the areas of computer vision and human-centred computing. Typical gaze prediction methods can be classified into bottom-up and top-down approaches. Bottom-up methods predict eye gaze from the low-level image features of the scene content such as intensity, colour, and orientation [6, 22]. For example, Itti et al. used multiscale colour, intensity, and orientation features extracted from the image to predict saliency map (density map of eye gaze distribution) [22] while Cheng et al. employed the global contrast features of the image to generate saliency map [6]. Top-down approaches take high-level features of the scene such as specific tasks and context information into consideration to predict eye gaze [4, 25]. For example, Borji et al. employed players' input such as 2D mouse positions and joystick buttons to predict their eye gaze [4] while Koulieris et al. used game state variables to predict users' eye gaze positions in video games [25]. In addition to the typical bottom-up and top-down approaches, recently some researchers took the eye-head coordination into consideration and attempted to predict eye gaze from human head movements [21, 45]. Specifically, Nakashima et al. proposed to use head directions as prior knowledge to improve the accuracy of bottom-up saliency prediction methods through simple multiplication of the predicted saliency map by a Gaussian head direction bias [38]. Sitzmann et al. employed users' head orientations to predict saliency maps for 360-degree images and achieved an accuracy that is on par with the performance of bottom-up saliency predictors [45]. Hu et al. proposed to use users' head rotation velocities to predict users' eye gaze positions in immersive virtual environments and achieved good performances in both free-viewing [20, 21] and task-oriented situations [17, 18]. However, existing works have only explored the effectiveness of head movements on the task of eye gaze prediction. In stark contrast, in this work we focus on the coordination of eye and full-body movements and investigate the effectiveness of full-body movements on generating realistic eye gaze.

3 ANALYSIS OF EYE-BODY COORDINATION

3.1 Gaze and Motion Data

To study the coordination between human eye gaze and full-body movements, we conducted a comprehensive analysis based on the only public motion capture datasets that also offer eye gaze information: MoGaze [26] and GIMO [51]. The MoGaze dataset contains eye gaze and full-body poses of 21 human joints from six people performing everyday *pick* and *place* activities in an indoor environment. GIMO dataset offers eye gaze and full-body poses of 23 human joints from 11 people performing daily activities in various indoor scenes. The activities include *resting* (*sitting* or *laying on objects*), *interacting with objects* (*touching*, *holding*, *stepping on*, *reaching to objects*), and *changing the state of objects* (*opening*, *pushing*, *transferring*, *throwing*, *picking up*, *lifting*, *connecting*, *screwing*, *grabbing*, *swapping objects*).

	Gaze	Head	Neck	Torso	Pelvis	Base
Gaze	1	0.92	0.84	0.64	0.59	0.63
Head	-	1	0.95	0.81	0.78	0.81
Neck	-	-	1	0.94	0.91	0.93
Torso	-	-	-	1	0.99	0.99
Pelvis	-	-	-	-	1	0.99
Base	-	-	-	-	-	1

(a) Gaze-body orientations in MoGaze

	Gaze	Head	Neck	Spine3	Spine2	Spine1	Pelvis
Gaze	1	0.93	0.89	0.84	0.77	0.84	0.72
Head	-	1	0.92	0.84	0.77	0.84	0.71
Neck	-	-	1	0.97	0.95	0.97	0.90
Spine3	-	-	-	1	0.98	0.99	0.94
Spine2	-	-	-	-	1	0.97	0.97
Spine1	-	-	-	-	-	1	0.93
Pelvis	-	-	-	-	-	-	1

(b) Gaze-body orientations in GIMO

Table 1: The cosine similarities between eye gaze directions and the directions of different body joints in the MoGaze and GIMO datasets. Gaze directions are strongly correlated with body orientations, especially with head directions. The directions of different body joints have strong correlations with each other.

3.2 Correlation between Eye Gaze and Body Orientations

We used the forward directions of human body joints available in the datasets to represent body orientations. Specifically, we represented body orientations in MoGaze using the forward directions of *head*, *neck*, *torso*, *pelvis*, and *base* and indicated body orientations in GIMO using the directions of *head*, *neck*, *spine3*, *spine2*, *spine1*, and *pelvis*. We used the cosine similarity to analyse the correlation between eye gaze and body orientations. Cosine similarity measures the similarity between two non-zero vectors by calculating the cosine of the angle between the vectors and produces a value in the range from -1 to $+1$, where -1 indicates perfect negative correlation, 0 denotes no correlation, and $+1$ represents perfect positive correlation. Table 1 summarises the cosine similarities between eye gaze and body orientations in the MoGaze and GIMO datasets. As the table shows, in both datasets eye gaze direction is strongly correlated with the directions of different body joints. In particular, eye gaze exhibits very high correlation with head direction, achieving a cosine similarity of 0.92 in MoGaze and 0.93 in GIMO. We also find that the directions of different body joints have very strong correlations with each other, e.g. neck and head directions have a cosine similarity of 0.95 in MoGaze and 0.92 in GIMO, indicating that there exists redundant information among these directions. Therefore, for simplicity, we suggest to use only head direction to generate human eye gaze rather than using all the body directions.

To investigate whether there exist time delays between head direction and eye gaze, we added different time intervals between head and gaze directions and further calculated their cosine similarities. We can see from Fig. 2 that head direction achieves its highest correlation with eye gaze at 100 *ms* in MoGaze and 0 *ms* in GIMO, indicating that there exists little or no time delay between head and eye movements.
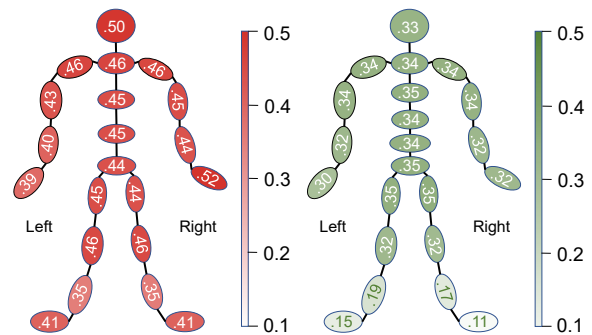
3.3 Correlations between Eye Gaze and Body Movements

To analyse the correlations between human eye gaze and human full-body movements, we calculated the velocities of different body joints and normalised these velocities to 3D unit vectors to represent the directions of body motions. We further calculated the cosine similarities between eye gaze and the directions of body motions
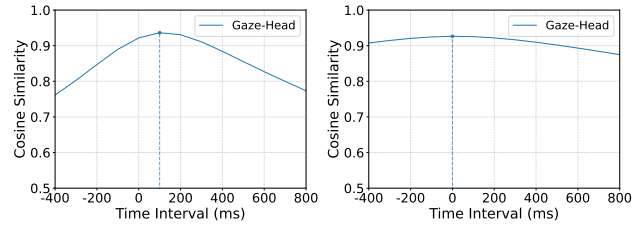
(a) Gaze-head direction in MoGaze (b) Gaze-head direction in GIMO

Figure 2: The cosine similarities between head and gaze directions at different time intervals in the (a) MoGaze and (b) GIMO datasets. Time interval refers to the time difference between head and gaze directions. The highest gaze-head correlation occurs at 100 *ms* in MoGaze and 0 *ms* in GIMO, suggesting that there is little or no time delay between head and eye movements.

(a) Gaze-body motions in MoGaze (b) Gaze-body motions in GIMO

Figure 3: The cosine similarities between eye gaze directions and the directions of body motions in the (a) MoGaze and (b) GIMO datasets. Eye gaze is strongly correlated with human full-body motions.

to measure their correlations. Fig. 3 shows the cosine similarities between eye gaze and full-body motions in the MoGaze and GIMO datasets, respectively. We can see that eye gaze directions have strong correlations with the motions of different body joints in both datasets.

To investigate any potential time delays between body motions and eye movements, we added different time intervals between body motions and gaze directions and further calculated their correlations. Specifically, for simplicity we first grouped all the human joints into three different body parts, i.e. Torso, Arm, and Leg. In the MoGaze dataset Torso consists of the body joints of *base*, *pelvis*, *torso*, *neck*, and *head* while in the GIMO dataset Torso contains the body joints of *pelvis*, *spine1*, *spine2*, *spine3*, *neck*, *head*, and *jaw*. In both datasets, Arm contains the body joints of *collar*, *shoulder*, *elbow*, and *wrist* while Leg includes *hip*, *knee*, *ankle*, and *foot*, where the left and right joints are averaged into one single joint, e.g. *left shoulder* and *right shoulder* are represented using *shoulder*. We then calculated the cosine similarities between eye gaze and the motions of different body parts as well as between eye gaze and the motions of specific joints. The correlation between gaze and a body part was computed using the mean of the cosine similarities between eye gaze and the specific joints within the body part. We can see from Fig. 4 that in both grouped body parts and specific body joints, the highest correlations consistently occur between current eye gaze and body motions in the near future, suggesting that there exists a noticeable time delay between body motions and eye movements.
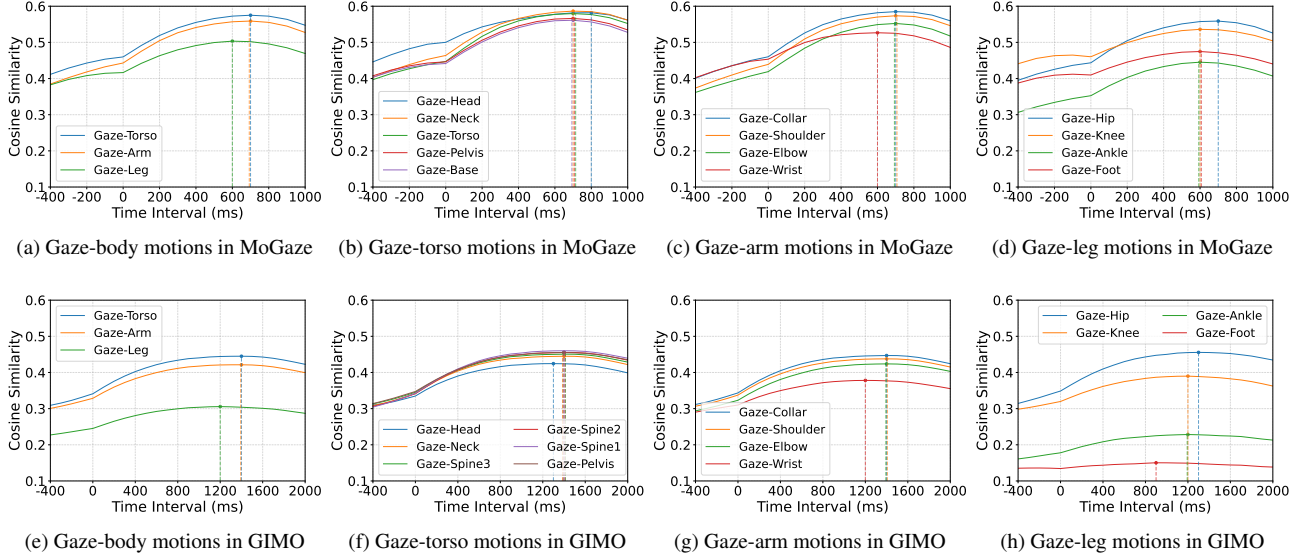
Figure 4: The cosine similarities between eye gaze and the motions of different body parts as well as between eye gaze and the motions of specific body joints at different time intervals in the (a-d) MoGaze and (e-h) GIMO datasets. Time interval refers to the time difference between body movements and eye gaze. The highest correlations consistently occur between current eye gaze and body motions in the near future (Time Interval > 0), indicating that there exists a significant time delay between body and eye movements.

3.4 Summary

Through comprehensive analysis, we find that eye gaze has very strong correlations with body orientations, especially with head directions, and there exists little or no time delay between head and eye movements. We also find that eye gaze is strongly correlated with human full-body motions and there exists a noticeable time delay between body and eye movements. These results suggest that head directions and full-body poses contain rich information about eye gaze and thus can be used to generate realistic eye movements.

4 POSE2GAZE: EYE-BODY COORDINATION MODEL

We define pose-based eye gaze generation as the task of generating a sequence of eye gaze directions $G_{t+1:t+T} = \{g_{t+1}, g_{t+2}, ..., g_{t+T}\} \in R^{3 \times T}$, where g is a 3D unit vector and T is the length of the target eye gaze sequence, from human body orientations and motions. We use a sequence of head directions $H_{t+1+\Delta t_h:t+T+\Delta t_h} = \{h_{t+1+\Delta t_h}, h_{t+2+\Delta t_h}, ..., h_{t+T+\Delta t_h}\} \in R^{3 \times T}$ to represent body orientations, where h is a 3D unit vector and Δt_h is the time interval between the input head directions and target eye gaze. We employ a sequence of the 3D positions of all human joints $P_{t+1+\Delta t_p:t+T+\Delta t_p} = \{p_{t+1+\Delta t_p}, p_{t+2+\Delta t_p}, ..., p_{t+T+\Delta t_p}\} \in R^{3 \times N \times T}$ to represent body motions, where N is the number of human joints and Δt_p is the time interval between the input body motions and target eye gaze. By setting different time intervals between the input body movements and the target gaze directions, our model can be trained to generate target eye gaze from past, present, or future body poses, respectively (see Sect. 5.1). Our method consists of three main components: a body orientation feature extraction module that extracts orientation features from head directions, a body motion feature extraction module that extracts motion features from full-body poses, and an eye gaze generation module that generates gaze directions from the extracted body orientation and motion features (see Fig. 5 for an overview of our method).

4.1 Body Orientation Feature Extraction

In light of the good performance of 1D convolutional neural networks for processing time series data [18,20], we employed three 1D CNN layers to extract body orientation features from the sequence of head directions. Specifically, we used two 1D CNN layers, each with 32 channels and a kernel size of three, to process the head direction sequence $H \in R^{3 \times T}$. Each CNN layer was followed by a layer normalisation (LN) and a Tanh activation function. After the two CNN layers, we used a 1D CNN layer with 32 channels and a kernel size of three, and a Tanh activation function to obtain the body orientation features $f_{ori} \in R^{32 \times T}$.

4.2 Body Motion Feature Extraction

Given the effectiveness of discrete cosine transform (DCT) for extracting temporal features from human pose data [33,35], we first employed DCT to encode human pose $P \in R^{3 \times N \times T}$ in the temporal domain using DCT matrix $M_{dct} \in R^{T \times T}$:

$$P_{dct} = PM_{dct}, \quad (1)$$

where $P_{dct} \in R^{3 \times N \times T}$ is the human pose after DCT transform. Considering the good performance of graph convolutional neural networks for processing human pose data [33,35], we propose two GCN blocks, i.e. a start GCN block and a residual GCN block, to extract motion features from the transformed pose data.

Start GCN Block The start GCN block first applies a temporal GCN (T-GCN) to extract the temporal features from the transformed pose data P_{dct}. The temporal GCN views the pose data as a fully-connected graph that contains T nodes corresponding to pose data at T time steps. It learns the weighted adjacency matrix $A^T \in R^{T \times T}$ of the fully-connected temporal graph and performs temporal convolution using

$$f_{temp} = P_{dct}A^T, \quad (2)$$

where $f_{temp} \in R^{3 \times N \times T}$ is the extracted temporal features. f_{temp} was then permuted to $f_{temp} \in R^{T \times N \times 3}$. A weight matrix $W^{start} \in R^{3 \times 16}$
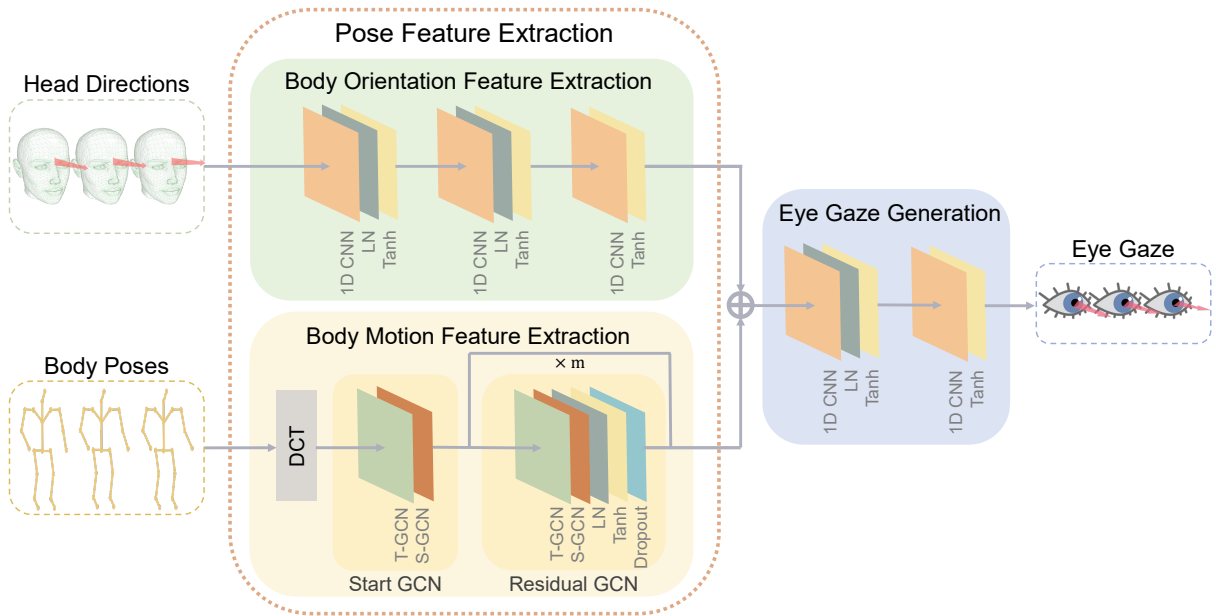
Figure 5: Architecture of the proposed *Pose2Gaze* model. *Pose2Gaze* first uses a 1D convolutional neural network to extract body orientation features from head directions, then applies a spatio-temporal graph convolutional neural network to extract the body motion features from human full-body poses, and finally employs a 1D convolutional neural network to generate human eye gaze from the extracted body orientation and motion features.

was applied to convert the input node features (3 dimensions) to latent features (16 dimensions):

$$f_{lat} = f_{temp} W^{start}, \qquad (3)$$

where $f_{lat} \in R^{T \times N \times 16}$ is the latent features. After the weight matrix, a spatial GCN (S-GCN) was applied to extract the spatial features. The spatial GCN views the latent features f_{lat} as a fully-connected graph that contains N nodes corresponding to N human joints. S-GCN learns the weighted adjacency matrix $A^S \in R^{N \times N}$ of the fully-connected spatial graph and performs spatial convolution using

$$f_{spa} = A^S f_{lat}, \qquad (4)$$

where $f_{spa} \in R^{T \times N \times 16}$ is the extracted spatial features. f_{spa} was further permuted to $f_{spa} \in R^{16 \times N \times T}$. The output of the spatial GCN is copied along the temporal dimension ($R^{16 \times N \times T} \to R^{16 \times N \times 2T}$) to enhance the features [33] and is then used as input to the residual GCN block.

Residual GCN Block The residual GCN block contains m GCN components with each component consisting of a temporal GCN that learns the temporal adjacency matrix $A_i^T \in R^{2T \times 2T}$, a weight matrix $W_i^{res} \in R^{16 \times 16}$ that extracts the latent features, a spatial GCN that learns the spatial adjacency matrix $A_i^S \in R^{N \times N}$, a layer normalisation, a Tanh activation function, and a dropout layer with dropout rate 0.3 to avoid overfitting. We set the number of GCN components m to 4 and added a residual connection for each GCN component to improve the network flow. We further cut the output of the residual GCN block in half in the temporal dimension to reduce the feature dimensions and obtained the spatio-temporal human body motion features $f_{mot} \in R^{16 \times N \times T}$.

4.3 Eye Gaze Generation

To generate eye gaze from the extracted body orientation and motion features, we first aggregated the body motion features f_{mot} along the

spatial dimension, i.e. concatenated the features of different body joints into a single motion feature ($R^{16 \times N \times T} \to R^{16N \times T}$). We then fused the extracted orientation and motion features by concatenating them along the spatial dimension and obtained $f \in R^{(16N+32) \times T}$. We finally used a 1D convolutional neural network to generate eye gaze from the fused features. Specifically, we used two CNN layers, each with a kernel size of three, to process the fused features. The first CNN layer has 64 channels and is followed by a layer normalisation and a Tanh activation function while the second CNN layer uses three channels and a Tanh activation function to generate the eye gaze. The generated eye gaze directions were finally normalised to unit vectors: $\hat{G}_{t+1:t+T} = \{\hat{g}_{t+1}, \hat{g}_{t+2}, ..., \hat{g}_{t+T}\} \in R^{3 \times T}$.

4.4 Loss Function

To train our model, we used the mean angular error between the generated eye gaze directions $\hat{G}_{t+1:t+T}$ and the ground truth gaze directions $G_{t+1:t+T}$ as our loss function:

$$\ell = \frac{1}{T} \sum_{j=t+1}^{t+T} \arccos(\hat{g}_j \cdot g_j). \qquad (5)$$

5 EXPERIMENTS AND RESULTS

We conducted extensive experiments to evaluate the performance of our gaze generation model. Specifically, we compared our model with state-of-the-art gaze prediction methods that estimate eye gaze from head movements on both the MoGaze and GIMO datasets. We tested these methods under three different generation settings, i.e. generating target eye gaze from past, present, and future body poses, respectively. We also performed an ablation study to evaluate the effectiveness of each component used in our model.

5.1 Experimental Settings

Datasets We evaluated our method on both the MoGaze and GIMO datasets since they are the two most established public datasets that offer both eye gaze and human full-body poses.

MoGaze contains eye gaze and full-body poses recorded at 30 fps from six people performing everyday *pick* and *place* actions. To evaluate our model's generalisation capability for different users, we performed a leave-one-person-out cross-validation: We trained on the data from five people and tested on the remaining one, repeated this procedure six times by testing for a different target person, and calculated the average performance across all six iterations. GIMO contains eye gaze and pose data (30 fps) from 11 people performing daily activities in various indoor scenes. To evaluate our model on GIMO, we used the default training and test sets provided by the authors [51], i.e. we used data from 12 scenes for training and data from 14 scenes (12 known scenes and two new scenes) for testing.

Evaluation Metric As is commonly used in gaze prediction [18, 20], we employed the mean angular error between the generated and ground truth gaze directions (see Equation 5) as the metric to evaluate model performance.

Baselines We compared our method with the following state-of-the-art gaze prediction methods that generate eye gaze from human head movements:

- *Head Direction*: *Head Direction* has been frequently used as a proxy for eye gaze due to the strong link between eye and head movements [20, 38, 45].
- *DGaze* [20]: *DGaze* predicts eye gaze from the sequence of head movements using a 1D convolutional neural network.
- *FixationNet* [18]: *FixationNet* extracts features from head movement sequence using a 1D convolutional neural network and combines the features with prior knowledge of gaze distribution to generate eye gaze directions.

Implementation Details We trained the baseline methods from scratch using their default parameters. To train our method, we used the Adam optimiser with an initial learning rate of 0.005 that we decayed by 0.95 every epoch. We used a batch size of 32 to train our method for a total of 50 epochs. We implemented our method using the PyTorch framework.

Generation Settings We set our model to generate 15 frames (corresponding to 500 ms) of eye gaze directions $G_{t+1:t+15} = \{g_{t+1}, g_{t+2}, ..., g_{t+15}\}$. We evaluated our method for three different generation tasks: Generating target eye gaze from past, present, and future body poses, respectively:

- *Generating Gaze from Past Poses*: We used the body poses and head directions in the past 15 frames $P_{t-14:t} = \{p_{t-14}, p_{t-13}, ..., p_t\}$ and $H_{t-14:t} = \{h_{t-14}, h_{t-13}, ..., h_t\}$ as input to generate the target eye gaze. This setting is equivalent to predicting human eye gaze in the future (gaze forecasting) [18, 20], which is important for a variety of applications including visual attention enhancement [10], dynamic event triggering [14], as well as human-human and human-computer interaction [37, 47].
- *Generating Gaze from Present Poses*: We used the body poses and head directions at the present time $P_{t+1:t+15} = \{p_{t+1}, p_{t+2}, ..., p_{t+15}\}$ and $H_{t+1:t+15} = \{h_{t+1}, h_{t+2}, ..., h_{t+15}\}$ as input to generate the corresponding gaze directions. This setting corresponds to estimating human eye gaze in real time [21, 25], which is key for a number of applications including gaze-contingent rendering [20, 21], gaze-based interaction [34], and gaze-guided redirected walking [48].
- *Generating Gaze from Future Poses*: Sect. 3.3 reveals that eye gaze has highest correlations with body motions in the near future and this implies that using future body poses may improve the performance of gaze generation. To evaluate the effectiveness of future body poses, we used the body poses in the future 15 frames $P_{t+16:t+30} = \{p_{t+16}, p_{t+17}, ..., p_{t+30}\}$ and the head directions at the present time $H_{t+1:t+15} = \{h_{t+1}, h_{t+2}, ..., h_{t+15}\}$ as input to generate the target eye gaze. We used real-time head

	Ours	*FixationNet* [18]	*DGaze* [20]	*Head Direction*
MoGaze-pick	**14.8°**	*18.2°*	18.3°	37.8°
MoGaze-place	**11.1°**	*15.2°*	15.3°	34.9°
MoGaze-all	**13.1°**	*16.8°*	16.9°	36.4°
GIMO-all	**18.6°**	21.1°	*20.6°*	23.1°

Table 2: Mean angular errors of different methods for generating eye gaze from past poses on the MoGaze and GIMO datasets. Best results are in bold while the second best are in italic.

directions because there exists little or no time delay between head and eye movements (Sect. 3.2). This setting can be seen as an offline processing way of generating realistic eye movements and is particularly important for creating and animating virtual humans [3, 41].

5.2 Gaze Generation Results

Generating Gaze from Past Poses Table 2 summarises the performances of different methods for generating eye gaze from past poses on both datasets. When evaluating on the MoGaze dataset, we calculated the mean angular errors on individual actions (*MoGaze-pick*, *MoGaze-place*) as well as on all the actions (*MoGaze-all*). We can see from the table that our method consistently outperforms the state-of-the-art methods on the MoGaze dataset. For *pick* and *place* actions, our method achieves an average improvement of 18.7% (14.8° *vs.* 18.2°) and 27.0% (11.1° *vs.* 15.2°) respectively in terms of mean angular error. For all actions on MoGaze, our method achieves an average improvement of 22.0% (13.1° *vs.* 16.8°) over the state of the art. The action labels for some recordings in the GIMO dataset are missing. Therefore, when evaluating on GIMO, we directly calculated the mean angular errors on all the actions (*GIMO-all*) and indicated the results in Table 2. We find that our method significantly outperforms the state of the art, achieving an average improvement of 9.7% (18.6° *vs.* 20.6°). We further performed a paired Wilcoxon signed-rank test to compare the performances of our method with the state-of-the-art methods and validated that the differences between our method and the state of the art are statistically significant ($p < 0.01$). The above results demonstrate that our method has a strong capability of generating eye gaze from past body poses.

Generating Gaze from Present Poses Table 3 summarises the mean angular errors of different methods for generating eye gaze from present body poses. We can see that on the MoGaze dataset our method significantly outperforms the state of the art on individual actions (*MoGaze-pick*, *MoGaze-place*) as well as on all the actions (*MoGaze-all*). Specifically, for *pick*, *place* and *all* actions, our method achieves an average improvement of 20.5% (10.5° *vs.* 13.2°), 20.5% (9.3° *vs.* 11.7°), and 20.8% (9.9° *vs.* 12.5°) respectively in terms of mean angular error. On the GIMO dataset, our method outperforms the state of the art with an average improvement of 17.5% (16.0° *vs.* 19.4°). A paired Wilcoxon signed-rank test was performed to compare the performances of our method with the state-of-the-art methods and the results indicated that the differences between our method and the state of the art are statistically significant ($p < 0.01$). Fig. 6 illustrates the generation results of different methods on the MoGaze and GIMO datasets. We can see that our method exhibits better generation performance than other methods (See supplementary video for more results). These results demonstrate that our method is able to generate realistic eye gaze from present body poses.

Generating Gaze from Future Poses Table 4 summarises the mean angular errors of different methods for generating eye gaze from future body poses. We can see that for *pick*, *place* and *all* actions on the MoGaze dataset, our method consistently outperforms the state of the art, achieving an average improvement of 25.8%

	Ours	FixationNet [18]	DGaze [20]	Head Direction
MoGaze-pick	**10.5°**	*13.2°*	13.4°	*17.6°*
MoGaze-place	**9.3°**	*11.7°*	12.1°	*16.2°*
MoGaze-all	**9.9°**	*12.5°*	12.8°	*16.9°*
GIMO-all	**16.0°**	19.5°	*19.4°*	19.4°

Table 3: Mean angular errors of different methods for generating eye gaze from present poses on the MoGaze and GIMO datasets.

	Ours	FixationNet [18]	DGaze [20]	Head Direction
MoGaze-pick	**9.8°**	*13.2°*	13.4°	*17.6°*
MoGaze-place	**8.6°**	*11.7°*	12.1°	*16.2°*
MoGaze-all	**9.2°**	*12.5°*	12.8°	*16.9°*
GIMO-all	**15.2°**	19.5°	*19.4°*	19.4°

Table 4: Mean angular errors of different methods for generating eye gaze from future poses on the MoGaze and GIMO datasets.

	Ours	w/o DCT	w/o S-GCN	w/o T-GCN	w/o Poses	w/o Head
Past	18.6°	**18.2°**	19.0°	18.3°	22.8°	23.2°
Present	**16.0°**	16.6°	17.3°	16.1°	20.7°	20.4°
Future	**15.2°**	16.4°	17.2°	16.0°	20.7°	19.5°

Table 5: Mean angular errors of different ablated versions of our method for generating eye gaze under different settings on GIMO.
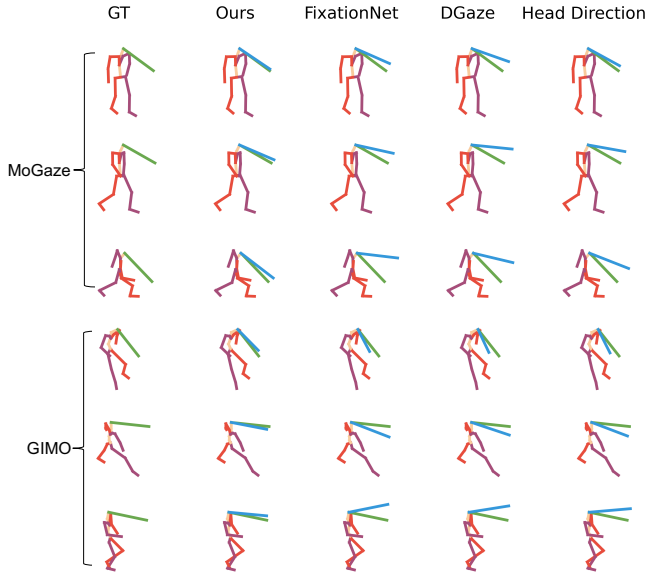

Figure 6: Results of different methods for generating eye gaze from present poses on MoGaze and GIMO. The green line indicates the ground truth while the blue line represents the generated eye gaze.

(9.8° *vs.* 13.2°), 26.5% (8.6° *vs.* 11.7°), and 26.4% (9.2° *vs.* 12.5°) respectively. On the GIMO dataset, our method outperforms the state of the art with an average improvement of 21.6% (15.2° *vs.* 19.4°) in terms of mean angular error. A paired Wilcoxon signed-rank test was conducted and the results validated that the differences between our method and the state of the art are statistically significant ($p < 0.01$). The above results demonstrate that our method has high performance in generating eye gaze from future body poses.

5.3 Summary

The results in above section demonstrate that our method significantly outperforms the state-of-the-art methods for three different generation tasks. Furthermore, by comparing our method's performances under different generation settings, we find that our method achieves its best performance in using future body poses (9.2° on MoGaze and 15.2° on GIMO), followed by using present body poses (9.9° on MoGaze and 16.0° on GIMO) and then using past poses (13.1° on MoGaze and 18.6° on GIMO). This result corresponds with our analysis in Sect. 3.3 that eye gaze has highest correlations with body motions in the near future and suggests that in offline applications where future pose is available, e.g. creating and animating virtual humans [3, 41], using future body poses could generate more realistic eye gaze.

Our model has smaller size than the state-of-the-art methods, containing only 0.17*M* trainable parameters while *DGaze* has 0.27*M* parameters and *FixationNet* contains 0.37*M* parameters. We implemented our model on an NVIDIA Tesla V100 SXM2 32GB GPU with an Intel(R) Xeon(R) Platinum 8260 CPU @ 2.40GHz and calculated its time costs. We find that our model requires only 35 ms to train per batch and 3 ms to test per batch, suggesting that our model is fast enough for practical usage.

5.4 Ablation Study

We finally performed an ablation study to evaluate the effectiveness of each component used in our model.

Effectiveness of Our Model Architecture   To evaluate the effectiveness of our model architecture, we evaluated different ablated versions of it that did not contain the *DCT*, *spatial GCN*, *temporal GCN*, the body poses input, and the head directions input, and retrained the ablated models. Table 5 summarises the performances of different ablated versions of our method for generating eye gaze on the GIMO dataset. We can see that our method consistently outperforms the ablated methods under different generation settings and the results are statistically significant (paired Wilcoxon signed-rank test, $p < 0.01$), thus underlining the effectiveness of our model architecture. One exception is that our method is not as good as the *w/o DCT* and *w/o T-GCN* versions in generating eye gaze from past body poses. This is probably because past body poses have weaker correlations with eye gaze than present and future body poses (Sect. 3.3), and thus the temporal features extracted from past body poses using *DCT* and *temporal GCN* are not as effective as that extracted from present and future poses.

Importance of Different Body Parts   We further evaluated the importance of different body parts for eye gaze generation. To this end, we re-trained our model using different body parts as input, i.e. only using the Torso part, Arm part, Leg part, as well as different combinations of these. Table 6 shows the performances of our method for generating eye gaze from different body parts on the GIMO dataset. As can be seen from the table, our method achieves significantly better performances than other versions (paired Wilcoxon signed-rank test, $p < 0.01$), validating that each body part used in our model can help improve the performance of eye gaze generation.

6 DISCUSSION

In this work we have made an important step towards understanding the correlation between eye and full-body movements in daily activities and generating eye gaze from full-body poses.

Eye-body Coordination   Our analyses on eye-body coordination in daily activities effectively guided the design of our model. Specifically, in the analysis of correlation between eye gaze and body orientations, we find that eye gaze has strong correlations with the orientations of different body joints, especially with head directions, and these body orientations are strongly correlated with each other (Table 1). Inspired by this, our model extracts body orientation features directly from head directions rather than all the body orientations (Sect. 4.1) because head direction itself contains

	Ours	Torso	Arm	Leg	Torso+Arm	Torso+Leg	Arm+Leg
Past	**18.6°**	20.7°	19.4°	19.7°	19.6°	19.6°	18.8°
Present	**16.0°**	17.8°	17.4°	18.0°	16.2°	17.0°	16.9°
Future	**15.2°**	18.6°	16.4°	18.3°	16.0°	16.7°	16.7°

Table 6: Mean angular errors of our method for generating eye gaze from different body parts under different settings on GIMO.

sufficient information for generating eye gaze. We also find that there exists little or no time delay between head and eye movements (Fig. 2). Therefore, in the task of generating gaze from future poses (Sect. 5.1), we used head directions at the present time to generate target eye gaze rather than using future head directions. In the analysis of correlation between eye gaze and body motions, we find that eye gaze is strongly correlated with full-body motions (Fig. 3). Therefore, our model extracts features from human full-body poses to generate realistic eye gaze (Sect. 4.2). We also find that there exists a noticeable time delay between full-body motions and eye gaze (Fig. 4). Inspired by this, we used future body poses as input to improve the performance of eye gaze generation in situations where future pose information is available (Sect. 5.2). The good performance of our model validated that our analyses are effective and significant for the design of eye-body coordination models.

Pose-based Gaze Generation Prior methods have typically generated eye gaze from head movements while our method generates eye gaze from full-body poses. Our method significantly outperforms prior methods on both the MoGaze and GIMO datasets for three different generation tasks (Table 2, Table 3, Table 4) and the ablation studies validated that each body part contributes to the performance of our method (Table 6). These results reveal the significant potential of human full-body poses for generating realistic eye movements and thus open the promising research direction of pose-based gaze generation.

Applications of Our Method We evaluated our method for three different generation tasks that are respectively linked to different kinds of applications (Sect. 5.1). The fact that our method outperforms the state-of-the-art methods by a large margin under all the three different generation settings (Table 2, Table 3, Table 4) demonstrates that our method has great potential for these numerous applications including dynamic event triggering [14], gaze-contingent rendering [20, 21], gaze-based interaction [9], as well as creating and animating virtual humans [3, 41]. In addition, with the development of motion capture and motion generation techniques [3, 15], it becomes increasingly easy to obtain human full-body poses. Our approach could be integrated with such motion capture and motion generation techniques to generate realistic eye and full-body movements simultaneously.

Limitations Despite these advances, we identified several limitations of our work that we plan to address in the future. First, we conducted our analysis and experiments using two public indoor datasets that contain eye and full-body movements in various daily activities. However, there exist some other interesting activities that are not covered by these datasets, e.g., narration or conversation actions [3]. No suitable gaze dataset exists yet, so the coordination of eye and full-body movements for these activities still remains to be explored. In addition, all activities in our datasets were performed in indoor environments and it remains to be seen whether eye-body coordination as characterised here also applies to outdoor scenarios. Furthermore, the activities we studied only cover the interaction between humans and objects and don't involve other interaction paradigms, e.g. interaction between two humans and interaction between a human and a social robot. Eye-body coordination in such interaction paradigms may be different and deserves to be studied in future work.

Future Work Besides overcoming the above limitations, many potential avenues of future work exist. First, it is well-known that human eye gaze is influenced by both the bottom-up scene content and the top-down tasks. Therefore, it will be interesting to analyse how the bottom-up and top-down factors influence the eye-body coordination. In addition, incorporating other modalities such as audio, text, or speech into our model may further boost our model's gaze generation performance. Finally, generating stylistic eye gaze, e.g. eye gaze that can convey different emotions [39], is an interesting avenue to extend our work.

7 CONCLUSION

In this work we were the first to explore the challenging task of generating realistic human eye gaze from human full-body poses. We first conducted a comprehensive analysis on the coordination of human eye and full-body movements in everyday activities and revealed that eye gaze is strongly correlated with head directions and also full-body motions. Based on these insights, we proposed a novel eye-body coordination model to generate eye gaze from head directions and full-body poses that outperformed the state-of-the-art methods by a large margin for three different generation tasks. Taken together, our work provides novel insights into eye-body coordination during daily activities and makes an important step towards more holistic, cross-modal generation of virtual agent behaviour.

REFERENCES

[1] A. U. Batmaz, A. K. Mutasim, M. Malekmakan, E. Sadr, and W. Stuerzlinger. Touch the wall: Comparison of virtual and augmented reality with conventional 2d screen eye-hand coordination training systems. In *Proceedings of the 2020 IEEE Conference on Virtual Reality and 3D User Interfaces*, pp. 184–193. IEEE, 2020.

[2] T. Baur, I. Damian, P. Gebhard, K. Porayska-Pomsta, and E. André. A job interview simulation: Social cue-based interaction with a virtual character. In *Proceedings of the 2013 International Conference on Social Computing*, pp. 220–227. IEEE, 2013.

[3] U. Bhattacharya, N. Rewkowski, A. Banerjee, P. Guhan, A. Bera, and D. Manocha. Text2gestures: A transformer-based network for generating emotive body gestures for virtual agents. In *Proceedings of the 2021 IEEE Virtual Reality and 3D User Interfaces*, pp. 1–10. IEEE, 2021.

[4] A. Borji, D. N. Sihite, and L. Itti. Probabilistic learning of task-specific visual attention. In *Proceedings of the 2012 IEEE Conference on Computer Vision and Pattern Recognition*, pp. 470–477. IEEE, 2012.

[5] R. Cañigueral and A. F. d. C. Hamilton. Being watched: Effects of an audience on eye gaze and prosocial behaviour. *Acta Psychologica*, 195:50–63, 2019.

[6] M.-M. Cheng, N. J. Mitra, X. Huang, P. H. Torr, and S.-M. Hu. Global contrast based salient region detection. *IEEE Transactions on Pattern Analysis and Machine Intelligence*, 37(3):569–582, 2015.

[7] D. DeVault, R. Artstein, G. Benn, T. Dey, E. Fast, A. Gainer, K. Georgila, J. Gratch, A. Hartholt, M. Lhommet, et al. Simsensei kiosk: A virtual human interviewer for healthcare decision support. In *Proceedings of the 2014 International Conference on Autonomous Agents and Multi-agent Systems*, pp. 1061–1068, 2014.

[8] N. F. Duarte, M. Raković, J. Tasevski, M. I. Coco, A. Billard, and J. Santos-Victor. Action anticipation: Reading the intentions of humans and robots. *IEEE Robotics and Automation Letters*, 3(4):4132–4139, 2018.

[9] A. T. Duchowski. Gaze-based interaction: a 30 year retrospective. *Computers and Graphics*, 73:59–69, 2018.

[10] M. S. El-Nasr, A. Vasilakos, C. Rao, and J. Zupko. Dynamic intelligent lighting for directing visual attention in interactive 3d scenes. *IEEE Transactions on Computational Intelligence and AI in Games*, 1(2):145–153, 2009.

[11] K. J. Emery, M. Zannoli, J. Warren, L. Xiao, and S. S. Talathi. Openneeds: A dataset of gaze, head, hand, and scene signals during exploration in open-ended vr environments. In *Proceedings of the 2021*

ACM Symposium on Eye Tracking Research and Applications, pp. 1–7, 2021.

[12] Y. Fang, R. Nakashima, K. Matsumiya, I. Kuriki, and S. Shioiri. Eye-head coordination for visual cognitive processing. *PloS One*, 10(3):e0121035, 2015.

[13] R. Giesen and A. Khan. *Acting and Character Animation: The Art of Animated Films, Acting and Visualizing*. CRC Press, 2017.

[14] J. Hadnett-Hunter, G. Nicolaou, E. O'Neill, and M. Proulx. The effect of task on visual attention in interactive virtual environments. *ACM Transactions on Applied Perception*, 16(3):1–17, 2019.

[15] D. Hasegawa, N. Kaneko, S. Shirakawa, H. Sakuta, and K. Sumi. Evaluation of speech-to-gesture generation using bi-directional lstm network. In *Proceedings of the 2018 International Conference on Intelligent Virtual Agents*, pp. 79–86, 2018.

[16] K. Higuch, R. Yonetani, and Y. Sato. Can eye help you? effects of visualizing eye fixations on remote collaboration scenarios for physical tasks. In *Proceedings of the 2016 CHI Conference on Human Factors in Computing Systems*, pp. 5180–5190, 2016.

[17] Z. Hu. Eye fixation forecasting in task-oriented virtual reality. In *Proceedings of the 2021 IEEE Conference on Virtual Reality and 3D User Interfaces Abstracts and Workshops*, pp. 707–708. IEEE, 2021.

[18] Z. Hu, A. Bulling, S. Li, and G. Wang. Fixationnet: forecasting eye fixations in task-oriented virtual environments. *IEEE Transactions on Visualization and Computer Graphics*, 27(5):2681–2690, 2021.

[19] Z. Hu, A. Bulling, S. Li, and G. Wang. Ehtask: recognizing user tasks from eye and head movements in immersive virtual reality. *IEEE Transactions on Visualization and Computer Graphics*, 2022.

[20] Z. Hu, S. Li, C. Zhang, K. Yi, G. Wang, and D. Manocha. Dgaze: Cnn-based gaze prediction in dynamic scenes. *IEEE Transactions on Visualization and Computer Graphics*, 26(5):1902–1911, 2020.

[21] Z. Hu, C. Zhang, S. Li, G. Wang, and D. Manocha. Sgaze: a data-driven eye-head coordination model for realtime gaze prediction. *IEEE Transactions on Visualization and Computer Graphics*, 25(5):2002–2010, 2019.

[22] L. Itti, C. Koch, and E. Niebur. A model of saliency-based visual attention for rapid scene analysis. *IEEE Transactions on Pattern Analysis and Machine Intelligence*, 20(11):1254–1259, 1998.

[23] C. Jiao, Z. Hu, M. Bâce, and A. Bulling. Supreyes: Super resolution for eyes using implicit neural representation learning. In *Proceedings of the 2023 Annual ACM Symposium on User Interface Software and Technology*, pp. 1–13, 2023.

[24] R. Kothari, Z. Yang, C. Kanan, R. Bailey, J. B. Pelz, and G. J. Diaz. Gaze-in-wild: a dataset for studying eye and head coordination in everyday activities. *Scientific Reports*, 10(1):1–18, 2020.

[25] G. A. Koulieris, G. Drettakis, D. Cunningham, and K. Mania. Gaze prediction using machine learning for dynamic stereo manipulation in games. In *Proceedings of the 2016 IEEE Virtual Reality*, pp. 113–120. IEEE, 2016.

[26] P. Kratzer, S. Bihlmaier, N. B. Midlagajni, R. Prakash, M. Toussaint, and J. Mainprice. Mogaze: A dataset of full-body motions that includes workspace geometry and eye-gaze. *IEEE Robotics and Automation Letters*, 6(2):367–373, 2020.

[27] T. Kucherenko, D. Hasegawa, G. E. Henter, N. Kaneko, and H. Kjellström. Analyzing input and output representations for speech-driven gesture generation. In *Proceedings of the 2019 ACM International Conference on Intelligent Virtual Agents*, pp. 97–104, 2019.

[28] T. Kucherenko, P. Jonell, S. Van Waveren, G. E. Henter, S. Alexandersson, I. Leite, and H. Kjellström. Gesticulator: A framework for semantically-aware speech-driven gesture generation. In *Proceedings of the 2020 International Conference on Multimodal Interaction*, pp. 242–250, 2020.

[29] M. E. Latoschik, D. Roth, D. Gall, J. Achenbach, T. Waltemate, and M. Botsch. The effect of avatar realism in immersive social virtual realities. In *Proceedings of the 2017 ACM Symposium on Virtual Reality Software and Technology*, pp. 1–10, 2017.

[30] H.-Y. Lee, X. Yang, M.-Y. Liu, T.-C. Wang, Y.-D. Lu, M.-H. Yang, and J. Kautz. Dancing to music. *Advances in Neural Information Processing Systems*, 32, 2019.

[31] J. Li, R. Kizilcec, J. Bailenson, and W. Ju. Social robots and virtual agents as lecturers for video instruction. *Computers in Human Behavior*, 55:1222–1230, 2016.

[32] M.-Y. Liao, C.-Y. Sung, H.-C. Wang, and W.-C. Lin. Virtual classmates: Embodying historical learners' messages as learning companions in a vr classroom through comment mapping. In *Proceedings of the 2019 IEEE Conference on Virtual Reality and 3D User Interfaces*, pp. 163–171. IEEE, 2019.

[33] T. Ma, Y. Nie, C. Long, Q. Zhang, and G. Li. Progressively generating better initial guesses towards next stages for high-quality human motion prediction. In *Proceedings of the 2022 IEEE Conference on Computer Vision and Pattern Recognition*, pp. 6437–6446, 2022.

[34] P. Majaranta and A. Bulling. *Eye Tracking and Eye-Based Human-Computer Interaction*, pp. 39–65. Springer Publishing London, 2014. doi: 10.1007/978-1-4471-6392-3_3

[35] W. Mao, M. Liu, and M. Salzmann. History repeats itself: Human motion prediction via motion attention. In *Proceedings of the 2020 European Conference on Computer Vision*, pp. 474–489. Springer, 2020.

[36] Meta. Meta horizon worlds. https://www.meta.com/horizon-worlds/.

[37] P. Müller, E. Sood, and A. Bulling. Anticipating averted gaze in dyadic interactions. In *Proceedings of the 2020 ACM International Symposium on Eye Tracking Research and Applications*, pp. 1–10, 2020. doi: 10.1145/3379155.3391332

[38] R. Nakashima, Y. Fang, Y. Hatori, A. Hiratani, K. Matsumiya, I. Kuriki, and S. Shioiri. Saliency-based gaze prediction based on head direction. *Vision Research*, 117:59–66, 2015.

[39] T. Randhavane, A. Bera, K. Kapsaskis, R. Sheth, K. Gray, and D. Manocha. Eva: Generating emotional behavior of virtual agents using expressive features of gait and gaze. In *Proceedings of the 2019 ACM Symposium on Applied Perception*, pp. 1–10, 2019.

[40] D. Roth, J.-L. Lugrin, D. Galakhov, A. Hofmann, G. Bente, M. E. Latoschik, and A. Fuhrmann. Avatar realism and social interaction quality in virtual reality. In *Proceedings of the 2016 IEEE Virtual Reality*, pp. 277–278. IEEE, 2016.

[41] K. Ruhland, C. E. Peters, S. Andrist, J. B. Badler, N. I. Badler, M. Gleicher, B. Mutlu, and R. McDonnell. A review of eye gaze in virtual agents, social robotics and hci: Behaviour generation, user interaction and perception: A review of eye gaze. *Computer Graphics Forum*, 34(6):299–326, 2015.

[42] V. Schwind, K. Wolf, and N. Henze. Avoiding the uncanny valley in virtual character design. *Interactions*, 25(5):45–49, 2018.

[43] L. Sidenmark and H. Gellersen. Eye, head and torso coordination during gaze shifts in virtual reality. *ACM Transactions on Computer-Human Interaction*, 27(1):1–40, 2019.

[44] L. Sidenmark and H. Gellersen. Eye&head: Synergetic eye and head movement for gaze pointing and selection. In *Proceedings of the 2019 Annual ACM Symposium on User Interface Software and Technology*, pp. 1161–1174, 2019.

[45] V. Sitzmann, A. Serrano, A. Pavel, M. Agrawala, D. Gutierrez, B. Masia, and G. Wetzstein. Saliency in vr: how do people explore virtual environments? *IEEE Transactions on Visualization and Computer Graphics*, 24(4):1633–1642, 2018.

[46] J. S. Stahl. Amplitude of human head movements associated with horizontal saccades. *Experimental Brain Research*, 126(1):41–54, 1999.

[47] J. Steil, P. Müller, Y. Sugano, and A. Bulling. Forecasting user attention during everyday mobile interactions using device-integrated and wearable sensors. In *Proceedings of the 2018 ACM International Conference on Human-Computer Interaction with Mobile Devices and Services*, pp. 1:1–1:13, 2018. doi: 10.1145/3229434.3229439

[48] Q. Sun, A. Patney, L.-Y. Wei, O. Shapira, J. Lu, P. Asente, S. Zhu, M. McGuire, D. Luebke, and A. Kaufman. Towards virtual reality infinite walking: dynamic saccadic redirection. *ACM Transactions on Graphics*, 37(4):1–13, 2018.

[49] Z. Ye, H. Wu, J. Jia, Y. Bu, W. Chen, F. Meng, and Y. Wang. Choreonet: Towards music to dance synthesis with choreographic action unit. In *Proceedings of the 2020 ACM International Conference on Multimedia*, pp. 744–752, 2020.

[50] Y. Yoon, W.-R. Ko, M. Jang, J. Lee, J. Kim, and G. Lee. Robots learn social skills: End-to-end learning of co-speech gesture generation for

humanoid robots. In *Proceedings of the 2019 International Conference on Robotics and Automation*, pp. 4303–4309. IEEE, 2019.

[51] Y. Zheng, Y. Yang, K. Mo, J. Li, T. Yu, Y. Liu, K. Liu, and L. J. Guibas. Gimo: Gaze-informed human motion prediction in context. In *Proceedings of the 2022 European Conference on Computer Vision*, 2022.